https://doi.org/10.5194/bg-2021-185
Preprint. Discussion started: 3 August 2021

Biogeosciences Discussions

Oxygen export to the deep ocean following Labrador Sea Water formation

Jannes Koelling[1], Dariia Atamanchuk[1], Johannes Karstensen[2], Patricia Handmann[2], and Douglas W.R. Wallace[1]

[1]Dalhousie University, Halifax, Nova Scotia, Canada
[2]GEOMAR Helmholtz Centre for Ocean Research, Kiel, Germany

Correspondence: Jannes Koelling (j.koelling@dal.ca)

Abstract. The Labrador Sea in the North Atlantic Ocean is one of the few regions globally where oxygen from the atmosphere can reach the deep ocean directly. This is the result of wintertime convection, which homogenizes the water column to a depth of up to 2000 m, and brings deep water undersaturated in oxygen into contact with the atmosphere. In this study, we analyze how the intense oxygen uptake during Labrador Sea Water (LSW) formation affects the properties of the outflowing deep western boundary current, which ultimately feeds the upper part of the North Atlantic Deep Water layer in much of the Atlantic Ocean.

Seasonal cycles of oxygen concentration, temperature, and salinity from a two-year time series collected by sensors moored at 600 m nominal depth in the outflowing boundary current at 53° N show that LSW is primarily exported in the months following the onset of convection, from March to August. During the rest of the year, properties of the outflow resemble those of Irminger Water, which enters the basin with the boundary current from the Irminger Sea. The input of newly ventilated LSW increases the oxygen concentration from 298 $\mu\mathrm{mol\,L^{-1}}$ in January to a maximum of 306 $\mu\mathrm{mol\,L^{-1}}$ in April. As a result of this LSW input, $1.57\times10^{12}\ \mathrm{mol\,year^{-1}}$ of oxygen are added to the outflowing boundary current, mostly during summer, equivalent to 49% of the wintertime uptake from the atmosphere in the interior of the basin. The export of oxygen from the subpolar gyre associated with this direct southward pathway of LSW is estimated to supply about 71% of the oxygen consumed annually in the upper North Atlantic Deep Water layer in the Atlantic Ocean between the equator and 50° N. Our results show that the formation of LSW is important for replenishing oxygen to the deep oceans, meaning that possible changes in its formation rate and ventilation due to climate change could have wide-reaching impacts on marine life.

1 Introduction

Much of the global supply of oxygen to the deep ocean is concentrated in a few key regions where near-surface water sinks to great depth and spreads away from its source region. This process ventilates the deep ocean, supplying oxygen to a vast volume of water that would otherwise be barren, and making it capable of sustaining life. One of the regions where such deep ocean ventilation occurs is the Labrador Sea, a semi-enclosed marginal sea nestled between eastern Canada and western Greenland. Here, strong wintertime atmospheric cooling leads to buoyancy loss of surface waters that lay above a weakly stratified water

https://doi.org/10.5194/bg-2021-185
Preprint. Discussion started: 3 August 2021


Biogeosciences Discussions

column, causing convective overturning that homogenizes the upper 1000-2000 m of the ocean (Marshall and Schott, 1999; Yashayaev, 2007). During the convection season, which typically lasts from January to April, deep water masses that are low in oxygen are continuously incorporated into the progressively deepening mixed layer, which leads to a decrease in near-surface oxygen. This results in severe air-sea gradients in oxygen concentration, which, together with extreme atmospheric conditions, drive intense uptake of oxygen during winter (Koelling et al., 2017; Wolf et al., 2018; Atamanchuk et al., 2020).

The climatological flow field in the Labrador Sea features a cyclonic boundary current entering at the southern tip of Greenland and exiting at the southwestern end of the Labrador Sea, with only a weak mean flow in the interior (Fig. 1). At mid-depth, the boundary current entering the basin carries Irminger Water, a water mass originating in the Atlantic ocean and modified in the subpolar gyre (Cuny et al., 2002; Pacini et al., 2020). The cyclonic circulation in the Labrador Sea is linked to a doming of isopycnals in the center of the basin, which supports deep convection in the interior (Marshall and Schott, 1999). Different types of eddies, such as Irminger Rings and convective eddies, compensate the annual mean surface heat loss in the interior, and help restratify the water column above the water mass formed during convection, known as Labrador Sea Water (LSW) (Eden and Böning, 2002; Straneo, 2006; de Jong et al., 2014; Rieck et al., 2019). Variability in atmospheric forcing, lateral fluxes of heat and freshwater, and the evolution of the mixed patch are main drivers for interannual variability in the depth of convection and in properties of LSW (Lazier, 1973; Yashayaev and Loder, 2016). Much of the research has been focused on the deep convection region in the interior of the basin, but it has been suggested that convection can also occur within the boundary current itself (Pickart et al., 1997; Palter et al., 2008). The densest water masses formed in the boundary current are similar to the ”classical” LSW formed in the interior, while convection over the continental slope forms a lighter water mass known as upper Labrador Sea Water, or uLSW (Pickart et al., 2002; Cuny et al., 2005). While the relative importance of boundary current convection is still uncertain, some model studies have suggested that it could account for a substantial fraction of the LSW that is eventually exported out of the region (Brandt et al., 2007; MacGilchrist et al., 2020).

The LSW formed each winter is one of the main water masses making up North Atlantic Deep Water, (NADW) (Lazier, 1973), and spreads throughout the Atlantic Ocean, both as part of the Deep Western Boundary Current (Molinari et al., 1998; Toole et al., 2017) and in the interior of the basin (Bower et al., 2009; Lozier, 2010). The signature of LSW is distinguishable in NADW properties far from the source region (Talley and McCartney, 1982; Rhein et al., 2004; Le Bras et al., 2017), including elevated oxygen concentrations compared to adjacent water masses (Atkinson et al., 2012). Although the importance of ventilation in the Labrador Sea on NADW properties is readily apparent from hydrographic data, the exact timing and mechanisms of the southward export of LSW from the subpolar gyre are not well established. Due to the weak mean currents in the center of the basin (see Fig. 1), some studies have suggested that much of the newly formed LSW remains in the interior for several years, with only a small fraction exported in the months following convection (Rhein et al., 2002; Straneo et al., 2003; MacGilchrist et al., 2021). On the other hand, there is evidence of a rapid export pathway of newly formed LSW, which may be associated with convection either within or close to the boundary current (Pickart et al., 1997; Brandt et al., 2007). An analysis from float data by Palter et al. (2008) showed that both interior and boundary convection can affect the properties of the outflowing boundary current, and suggested that eddies may play an important role in the input of newly formed LSW into the boundary current.

https://doi.org/10.5194/bg-2021-185
Preprint. Discussion started: 3 August 2021

Biogeosciences Discussions Open Access EGU

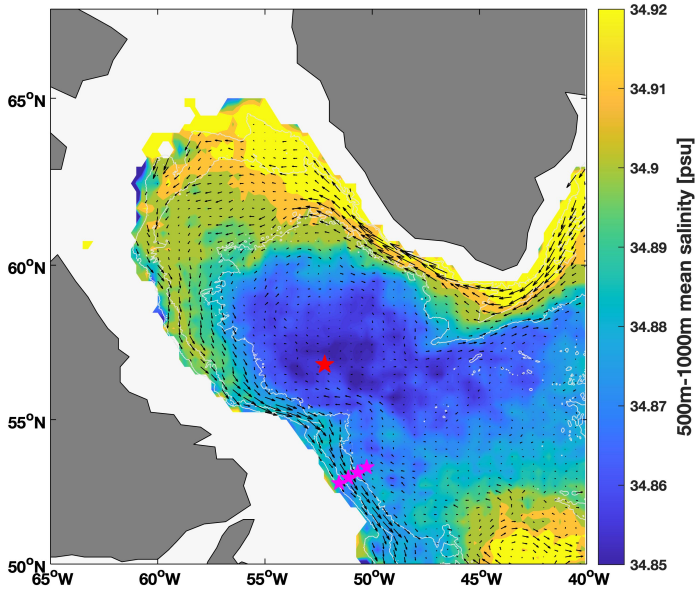

Figure 1. Mean salinity between 500 m and 1000 m in the Labrador Sea, calculated from all available Argo float profiles between 2000 and 2020. Gray lines show the 1000 m, 2000 m and 3000 m isobaths using data from Smith and Sandwell (1997), vectors show mean currents at 1000 m depth from Fischer et al. (2018), and symbols correspond to positions of the SeaCycler mooring (red) and the 53° N array (magenta).

In this study, we use a novel data set including moored oxygen concentration measurements from the outflowing boundary current at the southern exit of the Labrador Sea. The data are recorded at the 53° N array (Zantopp et al., 2017), which is part of the Overturning in the Subpolar North Atlantic Program, OSNAP (Lozier et al., 2017). We analyse annual cycles of oxygen, temperature, and salinity in order to investigate seasonal variations in the input of LSW into the boundary current. Our results reveal the important role of deep water formation in the Labrador Sea in supplying newly ventilated, oxygen-rich water to the global ocean.

2 Data and Methods

2.1 Moored sensor data

Data used in this study were collected from May 2016 to May 2018 on the 53° N array in the boundary current at the exit of the Labrador Sea, on moorings K7, K8, K9, and K10 (west to east in Fig. 1). Moorings have been deployed at the location since 1997, but in various configurations (Zantopp et al., 2017). In the present setup, each mooring is equipped with Aquadopp and RCM current meters and SeaBird SBE 37 instruments measuring conductivity, temperature (T), and pressure, which were also

https://doi.org/10.5194/bg-2021-185
Preprint. Discussion started: 3 August 2021

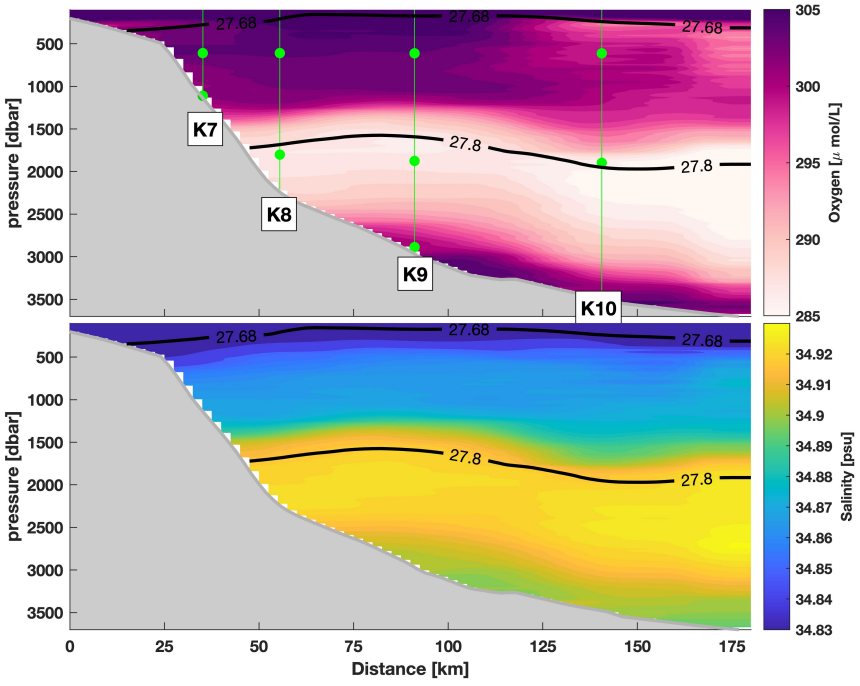

Figure 2. Oxygen and salinity sections along the array. Green symbols in the top panel show deployment locations of the oxygen sensors, which were co-located with T/S sensors. Only data from the instruments at 600 m depth are used in this study. The full coverage of current meters and T/S sensors is described in Zantopp et al. (2017). Black contours show the potential density range of 27.68 $\mathrm{kg\,m^{-3}} \leq \sigma\theta \leq$ 27.8 $\mathrm{kg\,m^{-3}}$ for Labrador Sea Water.

used to derive salinity (S). Observations are optimized to measure the strength and properties of the boundary current exiting the Labrador Sea (Zantopp et al., 2017). Since 2016, Aanderaa 4330O optodes (Aanderaa Data Instruments, AS) have been deployed at select depths alongside T/S sensors to measure dissolved oxygen (O_2) concentrations (Fig. 2a). We also use data from an Aanderaa 4330 oxygen optode mounted at 500 m depth on the SeaCycler mooring in the central Labrador Sea (see Fig. 1 for location). For the Seacyler optode, no co-located salinity data are available, and we estimate salinity used in Sec. 3.2 from a climatological T/S-relationship at 500 m calculated from Argo float data.

The deployment depths of the oxygen sensors on the 53° N array are shown in Fig. 2 along with mean oxygen and salinity sections along the array recorded with a Conductivity-Temperature-Depth (CTD) rosette during four mooring deployment cruises in 2014, 2016, 2018, and 2020. The majority of the O_2 sensors were deployed at nominal depths of approximately 600 m or 1900 m, chosen to represent the LSW core, and a depth near the bottom of the LSW layer. Only the sensors at 600 m depth are used in this study, and the deployment and calibration information for these sensors is summarized in Table 1. LSW is commonly defined in density space by a range of potential density σ_θ, with a lower boundary of 27.8 $\mathrm{kg\,m^{-3}}$, and an upper boundary of either 27.68 $\mathrm{kg\,m^{-3}}$ (Zantopp et al., 2017; Lozier et al., 2019) or 27.7 $\mathrm{kg\,m^{-3}}$ (Zou et al., 2020), the former of which is used as the definition of the LSW layer in this study. Within the LSW layer, oxygen concentrations are elevated

https://doi.org/10.5194/bg-2021-185
Preprint. Discussion started: 3 August 2021

Biogeosciences Discussions Open Access EGU

Mooring	Nominal deployment depth [m]	Mean potential density [$\mathrm{kg\,m^{-3}}$]	Optode Serial number	Drift [$\mu\mathrm{mol\,L^{-1}}$]
K7	608	27.72	052634	-5.8
K8	608	27.74	052631	-5.2
K9	610	27.74	052628	-2.5
K10	610	27.74	052626	-6.1

Table 1. Deployment location, depth and drift of the oxygen optodes during 2016–2018.

above 1200 m, and the mean salinity is 34.86. The low-oxygen core below LSW centered at about 2000 m depth coincides with a salinity maximum, which is indicative of Northeast Atlantic Deep Water (NEADW) (Yashayaev, 2007). Some authors differentiate between "upper" and "classical" Labrador Sea Water (Pickart et al., 1997), with the boundary between the two water masses typically at a potential density of $\sigma_\theta = 27.74\ \mathrm{kg\,m^{-3}}$ (Kieke et al., 2006). The mean potential density at 600 m depth is 27.72 $\mathrm{kg\,m^{-3}}$ for K7, and 27.74 $\mathrm{kg\,m^{-3}}$ for K8–K10 (Table 1), suggesting that sensors on these three moorings are near the interface between uLSW and cLSW.

The mean salinity of the boundary current in the LSW depth range decreases as it flows cyclonically around the basin (Fig. 1). At the 53° N array, the salinity is closer to values found in the interior Labrador Sea compared to the Greenland side, consistent with the view that there is significant input of LSW from the interior. However, the water here is still warmer and saltier than that found in the convective interior, suggesting that it also contains some remnant of Irminger Water (IW), which enters the Labrador Sea on the northern side in a mean core depth of about 500 m, and can be seen as a local salinity maximum near this depth (Pacini et al., 2020). In this study, we will focus on the variability of properties in this LSW layer, using data from the sensors mounted at about 600 m on the moorings, representing the full width of the boundary current from the shelf break area (K7, K8), via the core (K9), into the outer edge and recirculation regime (K10).

2.1.1 Sensor calibration

Temperature and salinity sensors were calibrated following the procedure outlined in Karstensen (2005). Briefly, the method involves attaching the sensors to a CTD rosette prior to and after each deployment, and comparing the data from the different instruments at certain stop depths with the CTD recording, which is calibrated with discrete bottle samples taken throughout the cruise.

Oxygen optodes were supplied with individual multipoint factory calibration, with an absolute accuracy of 1.5% or 2 $\mu\mathrm{mol\,L^{-1}}$ (Tengberg et al., 2006; Tengberg and Hovdenes, 2014), and powered by single-channel loggers (RBR Ltd.). The optodes were further calibrated against Winkler samples collected during CTD casts at the mooring locations during deployment and recovery cruises in 2016 and 2018 to correct for sensor drift. The drift of the sensors during deployment ranged from -2.5 $\mu\mathrm{mol\,L^{-1}}$ to -6.2 $\mu\mathrm{mol\,L^{-1}}$, or 0.4–1% per year (see Table 1).

https://doi.org/10.5194/bg-2021-185
Preprint. Discussion started: 3 August 2021

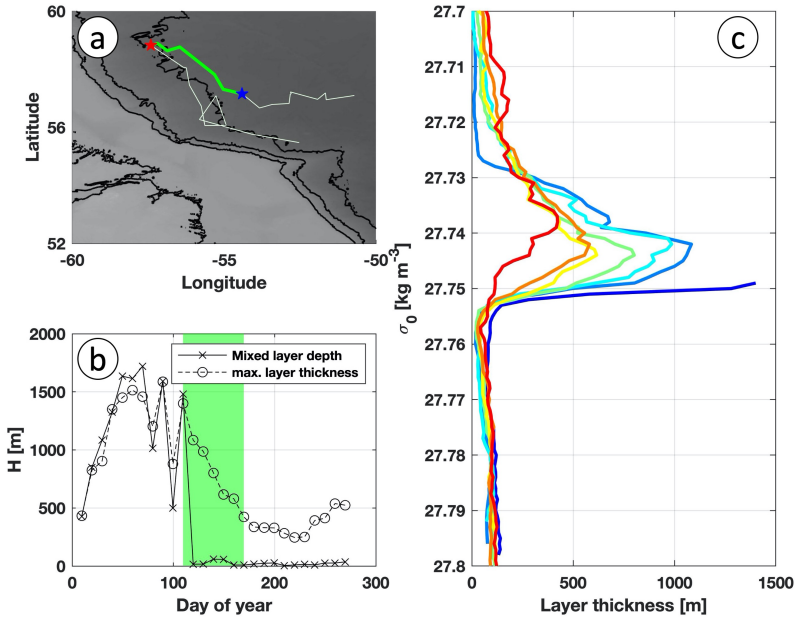

Figure 3. Example of Argo data used to track export of LSW, from float ID 6902589. a) Trajectory showing latest deep mixed layer measurement (blue star) and export location (red star). b) Time series of mixed layer depth and maximum layer thickness, with green shading highlighting the time from convection to export. c) Consecutive profiles of layer thickness in density space, going from convection (blue) to export (red).

Initially, the time series show mixed layer depth and maximum layer thickness varying in concert, as the thickest layer is the actively convecting mixed layer. This is also evident in the last profile measuring convection, as the maximum layer thickness is found at the lowest density measured. Subsequently, the mixed layer depth decreases to almost zero, indicating surface restratification, but a maximum in layer thickness remains. In the profiles, this can be seen as lower-density water accumulating above the maximum around $\sigma_\theta = 27.74\ kgm^{-3}$. The magnitude of the maximum decreases through mixing with surrounding water, but it is still detectable in the profile as the float enters the boundary current.

2.2 Tracking Labrador Sea Water formation and export

To evaluate the export of LSW out of the Labrador Sea, we use data from the Argo program (Roemmich et al., 2009), which are freely available online, to investigate convection regions and LSW export in Sect. 3.1. The data used here were downloaded from coriolis.eu.org, and span the 2000-2020 period (Argo (2020), https://doi.org/10.17882/42182#77634), and longitude and latitude ranges of 65°W–40°W, 50°N–65°N, giving a total of 41165 temperature and salinity profiles from 568 floats. The profile data are used to calculate mixed layer depths based on a density difference of $\Delta\sigma_\theta = 0.01\ \mathrm{kg\,m^{-3}}$ from the shallowest measurement. After the last convective profile for each season, defined here as a mixed layer depth exceeding 600 m, we track the trajectory until the float is exported. We define export as a float crossing the 3000 m isobath and subsequently staying in the

https://doi.org/10.5194/bg-2021-185
Preprint. Discussion started: 3 August 2021

boundary current for at least 2 out of the next 3 profiles thereafter, similar to definitions used in previous studies (Palter et al., 2008; Georgiou et al., 2020).

During a typical Argo cycle, floats park at a depth of either 1000 m or 1500 m for 10 days before descending to 2000 m, measuring a profile to the surface and staying there to transmit the data, which typically last about one hour, but can be as much as 12 hours for older float models (Lebedev et al., 2007). As a result, the floats are not strictly following a water parcel, as vertically sheared currents can carry them away from the water mass they had been advected with at depth. To ensure that floats used for the export calculation are following Labrador Sea Water, we use layer thickness measurements to track them. Layer thickness is inversely proportional to the vertical density gradient, and newly formed Labrador Sea Water is readily detected as a maximum (Yashayaev and Loder, 2016). An example of layer thickness measurements from a float measuring convection in the interior of the basin and subsequently entering the boundary current on the southwestern side is shown in Fig. 3. After the initial profile measuring a deep mixed layer, surface restratification and mixing lead to a decrease in maximum layer thickness, but the signature of LSW remains detectable. To ensure that only floats moving with newly formed LSW were used, we discarded data from floats with changes in maximum layer thickness of more than 50% between consecutive profiles. As a result, data from about 12% of all floats measuring convection were omitted from the analysis, but the findings discussed in Sect. 3.1 do not change qualitatively if all float data are used instead.

3 Results

Time series of oxygen at 600 m nominal depth (Fig. 4) show an overall similar picture at all sites: Starting in February–March, high-frequency oxygen variability intensifies, and mean oxygen concentrations increase by around 10 $\mu\mathrm{mol\,L^{-1}}$, remaining elevated during spring. Beginning in July, oxygen concentrations decrease slowly throughout the year, and the short-term variability subsides, until the next increase the following winter. The shift in oxygen concentrations appears to occur in concert with changes in temperature and salinity (Fig. 5). T/S changes occur largely along isopycnals, meaning that the effect of T and S variations on density compensate each other. Correlation between T and O_2 is high for all of the sites (between -.78 and -.94). Although some of this can be explained by solubility changes, which are dependent on temperature (Garcia and Gordon, 1992), correlations between oxygen saturation and temperature are still $\geq .5$, indicating that concentration changes are not simply due to temperature-driven solubility differences. Instead, the changes appear to be associated with the presence of different water masses, with warmer, saltier and lower oxygen water observed in fall and early winter, and colder, fresher, higher O_2 water in late winter and spring. The majority of the T/S measurements lie roughly along a mixing line between typical endmembers for LSW and IW (see Fig. 5 for reference). The clustering of measurements between these two endmembers suggests that variability of properties at 53° N, including oxygen, is chiefly controlled by changes in the fraction of each source water mass found in the boundary current.

In the following sections, we will analyse the main features of the time series in more detail, discussing first the initial oxygen increase in February and March, and associated higher-frequency variability, using data from the K9 mooring (Sect. 3.1). This is followed by an analysis of a complete seasonal cycle of oxygen concentration at K9, covering convection and the

https://doi.org/10.5194/bg-2021-185
Preprint. Discussion started: 3 August 2021

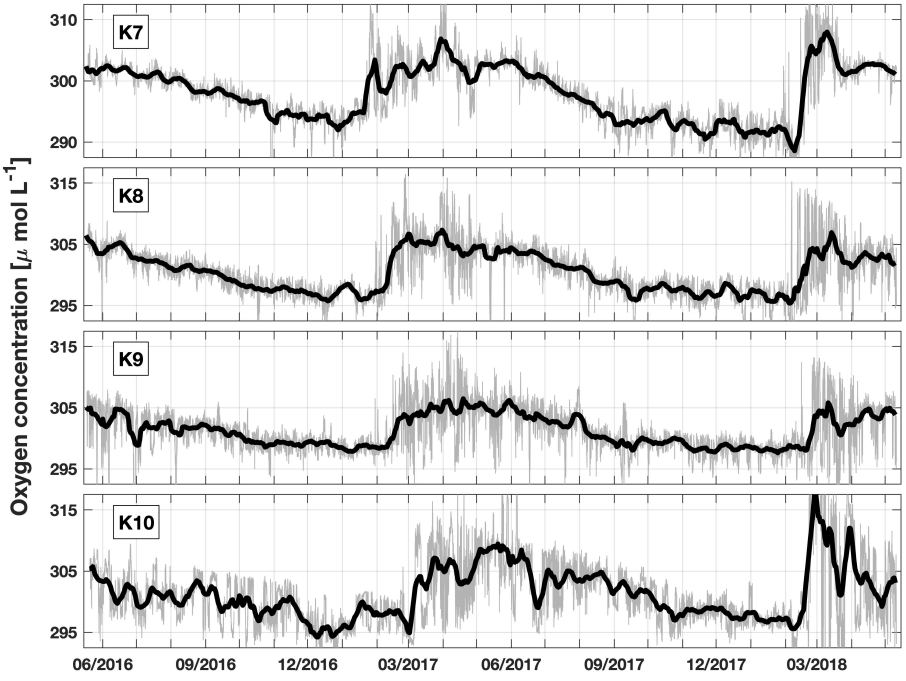

Figure 4. Time series of oxygen concentration at 610 m for K7, K8, K9 and K10 (top to bottom). Gray lines show original 15-minute data, and black lines show time series filtered with a 10-day running mean.

following restratification period in 2016–2017 (Sect. 3.2), and a brief analysis of the differences between the moorings (Sect. 3.3).

3.1 High-frequency oxygen variability in February–April

As oxygen concentrations at the mooring sites begin to increase in late February, there is a concurrent increase in the spread of the measurements (Fig. 4). During the months of February, March, and April, oxygen concentrations at K9 oscillate between values typical of the months prior, between 297 $\mu\mathrm{mol\,L^{-1}}$ and 301 $\mu\mathrm{mol\,L^{-1}}$, and higher values ranging from 305 $\mu\mathrm{mol\,L^{-1}}$ to 315 $\mu\mathrm{mol\,L^{-1}}$, which subsequently persist until late June. During these months, the spread between the minimum and maximum values measured in a single day can be as much as 15 $\mu\mathrm{mol\,L^{-1}}$, and the standard deviation increases from 1.1 $\mu\mathrm{mol\,L^{-1}}$ for the 3-month period from 1 November, 2016 to 31 January, 2017 to 4.2 $\mu\mathrm{mol\,L^{-1}}$ for 1 February, 2017 to 30 April, 2017.

This wide spread in the measured oxygen concentrations is also reflected in differing temperature and salinity properties for a 20-day period in February (Fig. 6). As for the overall dataset, the highest oxygen values occur at the lowest temperatures and salinities. Starting from a cluster of points with higher temperatures and salinities for February 7 to February 12, water with properties of LSW begins to emerge in the following days, and by February 27, some of the measured T/S values are similar to those found in the center of the basin during convection (see also Fig. 5). During this time, much of the annual range of temperature, salinity, and oxygen properties found in the 2–year record is observed within just 20 days. This stark

https://doi.org/10.5194/bg-2021-185
Preprint. Discussion started: 3 August 2021

Biogeosciences
Discussions
Open Access
EGU

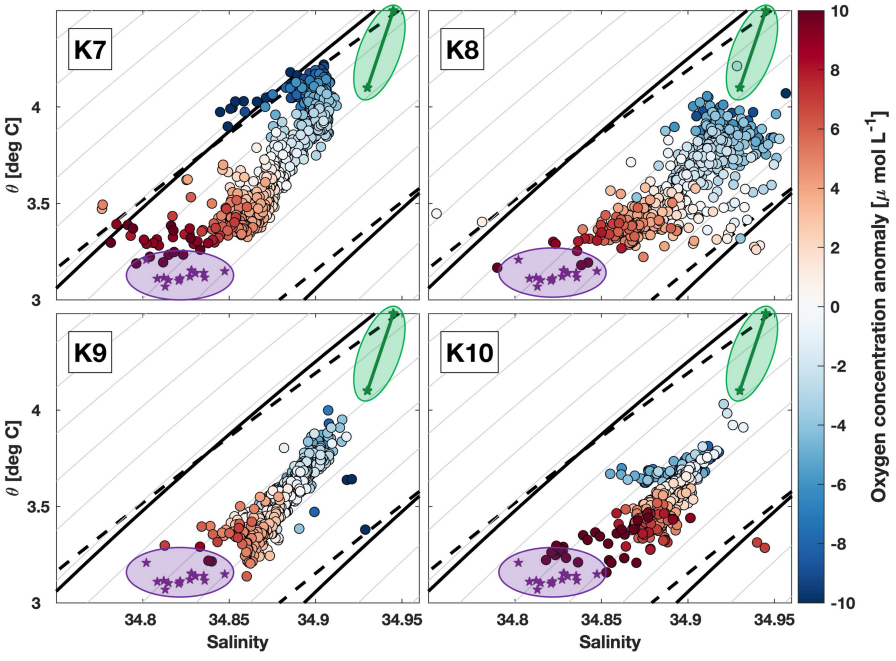

Figure 5. Temperature and salinity diagrams at about 600 m nominal depth from all four boundary current moorings. Colors correspond to oxygen anomalies from -10 $\mu\mathrm{mol\,L^{-1}}$ (blue) to +10 $\mu\mathrm{mol\,L^{-1}}$ (red). Purple stars and shading show values from the wintertime mixed layer at the SeaCycler mooring in the interior Labrador Sea (Atamanchuk et al., 2020), and green symbols and shading show typical wintertime conditions of Irminger Water near Greenland, taken from Pacini et al. (2020). Potential density (σ_θ) contours are drawn with a spacing of 0.025 $\mathrm{kg\,m^{-3}}$, black solid contours show densities of σ_θ = 27.68 $\mathrm{kg\,m^{-3}}$ and σ_θ = 27.8 $\mathrm{kg\,m^{-3}}$, and black dashed contours show density referenced to 600 dbar, σ_{600} = 30.46 $\mathrm{kg\,m^{-3}}$ and σ_{600} = 30.58 $\mathrm{kg\,m^{-3}}$.

heterogeneity of properties may suggest that newly formed LSW is rapidly exported out of the Labrador Sea in February, and some of it is transported with the boundary current without much mixing with the surrounding water.

Despite the early arrival of newly ventilated water and drastic variability in properties, there is little variability in density. This speaks against the source being local convection at the 53° N array, as property changes forced by surface buoyancy loss would have a larger diapycnal signature. This is also supported by the near-surface density measurements that are available at about 50 m depth at K7 and K8 (not shown), which do not exhibit signs of a static instability associated with convective overturning, as vertical density gradients stay above the commonly used threshold of $\Delta\sigma_\theta = 0.01 kgm^{-3}$. Instead, we conclude that the water must be advected to the 53° N array from upstream. The observations are consistent with LSW being formed in the interior of the basin and entering the boundary current along isopycnals (Georgiou et al., 2020). Convection can also occur in the boundary current itself, with surface forcing eroding stratification as it rounds the basin (Pickart et al., 2002; Cuny et al., 2005; Palter et al., 2008). Although there is no evidence of local convection in the 53° N data, convection may have occurred further upstream in the boundary current, which could explain the observed changes.

https://doi.org/10.5194/bg-2021-185
Preprint. Discussion started: 3 August 2021

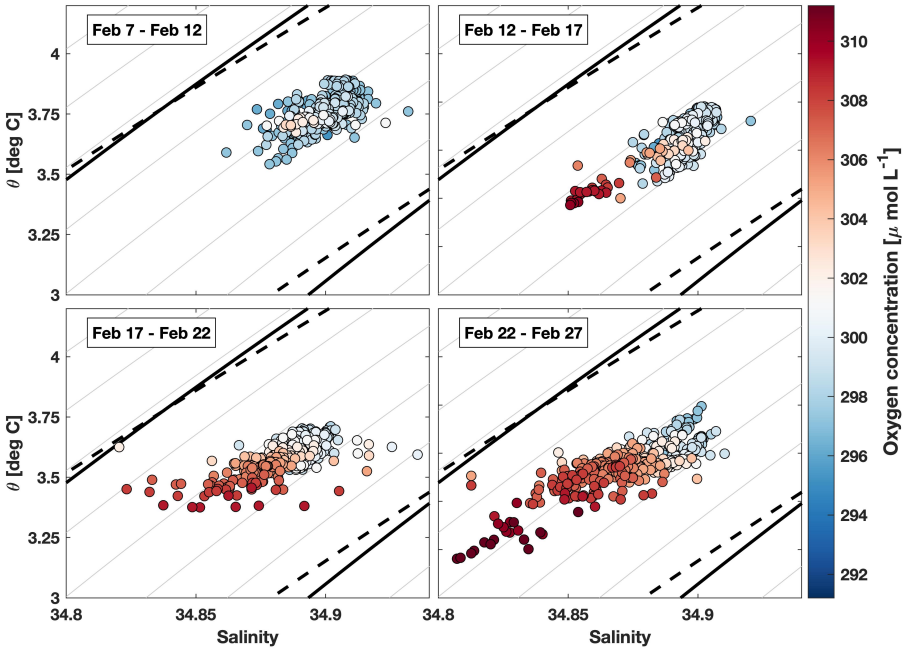

Figure 6. T/S properties at K9 at 15-minute resolution for four consecutive 5-day periods during the initial oxygen increase in February. Colors correspond to oxygen concentration. Potential density (σ_θ) contours are drawn with a spacing of 0.025 $\mathrm{kg\,m^{-3}}$, solid black contours show densities of σ_θ = 27.68 $\mathrm{kg\,m^{-3}}$ and σ_θ = 27.8 $\mathrm{kg\,m^{-3}}$, and black dashed contours show density referenced to 600 dbar, σ_{600} = 30.46 $\mathrm{kg\,m^{-3}}$ and σ_{600} = 30.58 $\mathrm{kg\,m^{-3}}$. Note changed axes ranges compared to Figure 5.

In order to identify the source of the LSW arriving at 53° N in February, we use data from Argo floats to investigate the timing of convection and export. Fig. 7 shows the fraction of profiles within 50 km of each $0.5° \times 0.5°$ bin that measured mixed layers deeper than 600 m in the Holte et al. (2017) Argo mixed layer depth database. The most salient feature is a large area of deep mixed layers in the interior of the basin, near the mixed patch often defined as the LSW formation region (Lazier, 1973; Yashayaev, 2007; Atamanchuk et al., 2020). The area extends eastward and indicates a major interior ocean spreading pathway that connects the Labrador Sea and Irminger Sea (Talley and McCartney, 1982; Sy et al., 1997; Fischer et al., 2018; Zunino et al., 2020). Another region of increased occurrence of deep mixed layers is found inshore of the 3000 m isobath near 55° W, close to where Pickart et al. (2002) first reported evidence of convection in the boundary current. No mixed layers deeper than 600 m are found in the boundary current south of 55° N, consistent with our findings from the mooring data that convection did not occur locally at 53° N.

Also shown in the figure are convection locations for all floats from the 2000–2020 period from the Argo data described in Sect. 2.2, using the last profile measuring a mixed layer deeper than 600 m. The points generally line up with the mean picture from the Holte et al. (2017) data, but are more concentrated towards the sides of the patch, likely due to continued modification

https://doi.org/10.5194/bg-2021-185
Preprint. Discussion started: 3 August 2021

during convection. Overall, the majority of the profiles measuring convection in both datasets are in the interior, with most of the floats with deep mixed layers inshore of the 3000 m isobath found immediately adjacent to the interior patch.

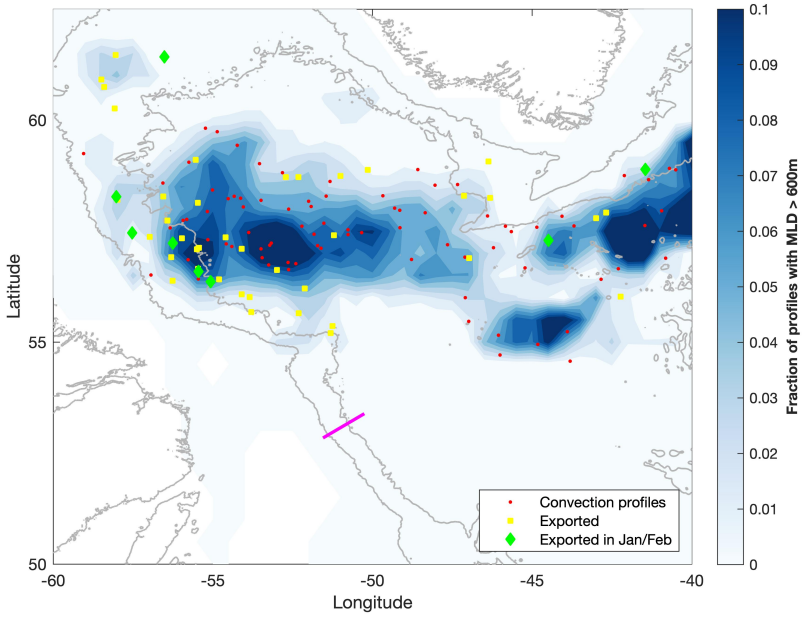

Figure 7. Fraction of total profiles from Holte et al. (2017) database with mixed layer depth over 600 m. Grey contours show the 2000 m and 3000 m isobaths, and the magenta line shows the 53° N array. Overlaid are the convection locations for each float measuring convection as defined in Sect. 2.2, differentiating between floats that are not exported within the same year (red dots), those that are exported (yellow squares), and those that are exported in either January or February (green diamonds).

A quantitative analysis of the relative importance of the different formation regions is beyond the scope of this study, as the Lagrangian nature of Argo floats results in undersampling of fast-flowing boundary currents relative to regions with weak currents like the interior Labrador Sea. Nonetheless, our data set reveals some qualitative features about the differences between convection in the interior and within the boundary current. The profile locations in Fig. 7 are color coded by whether or not the float is exported during the same year, as defined in Sect. 2.2. About half of the floats measuring convection in the interior remain there until the following convective season, consistent with model studies showing that newly formed LSW can remain in the interior for several seasons (Straneo et al., 2003; Georgiou et al., 2020). Conversely, most of the profiles measuring deep mixed layers inshore of the 3000 m isobath stay within the boundary current afterwards, suggesting that a larger fraction of LSW formed in the boundary current is exported compared to LSW formed in the interior. Moreover, out of the more than 100 floats measuring convection to depths exceeding 600 m, only a handful are subsequently found inshore of the 3000 m isobath in the months of January and February. The convection location of these floats is highlighted in Fig. 7 by green diamonds. The floats found in the boundary current during this time either measured convection very close to the 3000 m isobath, which

https://doi.org/10.5194/bg-2021-185
Preprint. Discussion started: 3 August 2021

allows for a quicker export timescale, or convection within the boundary current region (such that no export is necessary). This suggests that the initial arrival of the high oxygen signal at the moorings in February is likely to be a result of convection within, or close to, the boundary current.

3.2 Seasonal Cycle

To investigate the broader-scale variability over a whole year, we look at the relation between oxygen and temperature and salinity for the period of December 2016 to December 2017, covering a full annual cycle including convection and restratification. Fig. 8 shows the evolution of the oxygen concentration throughout the year in the form of monthly histograms with a bin size of 1 $\mu\mathrm{mol\,L^{-1}}$. The color for each bin shows the mean spiciness (π), which is a measure of temperature and salinity changes along an isopycnal (Flament, 2002), and is used here as a water mass index to quantify the relative contribution of the two endmember water masses, LSW and IW. Fig. 8 uses data from the K9 mooring, and results from all other moorings are discussed in the following section.

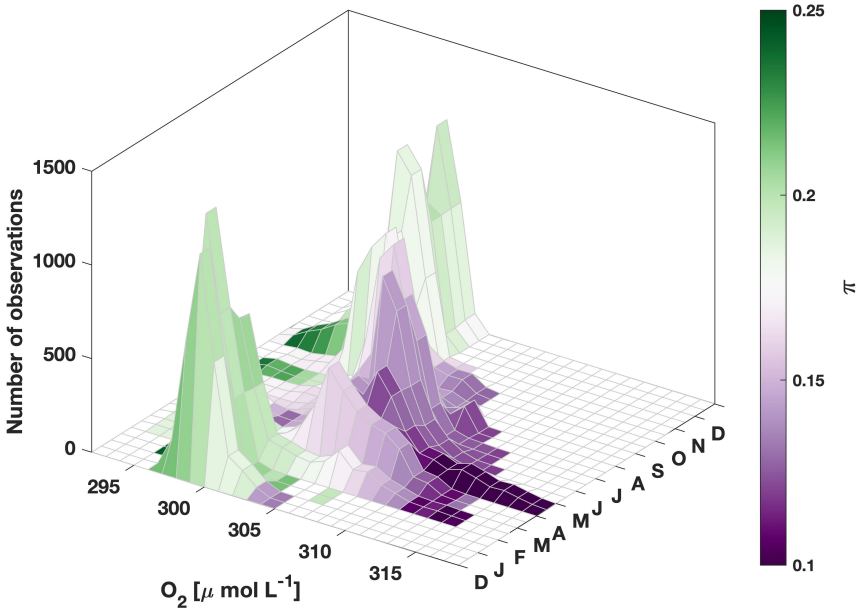

Figure 8. Monthly histogram of oxygen from December 2016 to December 2017 at about 600 m depth at K9. Colors show the mean spiciness of each O_2 bin, with lower values corresponding to LSW and higher values to IW (see text for definition).

Overall, the seasonal cycle is marked by a shift from water with lower oxygen and T/S properties closer to those of Irminger Water towards high-oxygen Labrador Sea Water, which is most prevalent in the months of March–July. In January, the bulk of the measurements at K9 show similar properties. The most abundant class of oxygen values is at 298 $\mu\mathrm{mol\,L^{-1}}$, and the water mass index shows higher temperatures and salinities, indicative of IW most likely advected from upstream within the

https://doi.org/10.5194/bg-2021-185
Preprint. Discussion started: 3 August 2021


Biogeosciences Discussions Open Access EGU

boundary current. There is little spread around this mean value, with almost all measurements falling in the range of 297-301 $\mu mol\,L^{-1}$. In the month of February, measurements showing water with oxygen concentrations around 297 $\mu mol\,L^{-1}$ still make up the majority of values seen in the record, but the number of observations in the central bin decreases. Moreover, a smaller secondary peak emerges at a concentration of 306 $\mu mol\,L^{-1}$, with lower mean temperature and salinity values, and there is a wide spread of oxygen concentrations measured, ranging from 297 $\mu mol\,L^{-1}$ to 315 $\mu mol\,L^{-1}$. This is in line with the assumption that at this time, all of the LSW reaching 53° N was recently convected, allowing for less time to mix with the surrounding boundary current waters and resulting in the larger spread in properties (see Sect. 3.1).

In the following months, the LSW peak becomes more pronounced and replaces the class of higher temperature and salinity water with low O2 as the most abundant water mass. In April, the most commonly measured O2 value is at its annual maximum of 306 $\mu mol\,L^{-1}$. By May, a wider range of export and mixing time scales results in a more homogenized boundary current, as evidenced by the higher number of observations in the central O2 bin. With the increased input of newly formed LSW, the T/S properties are at the opposite end of the water mass index (π) compared to December–February. After June, oxygen concentrations are beginning to decrease again, with a concurrent increase in T and S, indicative of a larger fraction of IW. Only isolated instances of elevated oxygen concentrations are observed at K9 by August and September, as the water at 600 m depth becomes warmer, saltier, and less oxygenated. In the autumn months, the signature of LSW has all but disappeared, with water found at the mooring once more resembling the properties of IW, before the cycle begins anew the following winter.

Fig. 9 compares the seasonal oxygen cycle at K9 from Fig. 8 to the seasonal cycle of LSW input into the boundary current, and a partial seasonal cycle at 500 m depth from the SeaCycler mooring in the interior of the basin (see Fig. 1 for location). The input of LSW into the boundary current is an average over all years from the float data used in Sect. 3.1, and includes both convection within the boundary current and LSW entering the boundary current from the interior. LSW input begins to increase in late January, peaks in April, and decreases to almost zero in July, broadly consistent with the amount of LSW leaving the interior derived from measurements of layer thickness (Yashayaev and Loder, 2016), and rates of boundary-interior exchange inferred from heat content changes (Straneo, 2006). The curve has a similar shape to the seasonal cycle of the most commonly measured O_2 concentration at K9, shown as a black line in the figure, but the two are shifted relative to one another: The O_2 concentration maximum increases in March, reaches its peak in April, and then stays at a similar level until June, before starting to decrease in July and August, lagging the increase in LSW input by about 1–2 months. At the SeaCycler mooring, the oxygen concentration begins to increase in January and February, and remains elevated until the end of the available record in June 2017. Oxygen concentrations in the interior before January are lower than those at 53° N during March–July, confirming that the increased oxygen levels of the outflowing boundary current must be associated with recently convected water, rather than older LSW.

Typical current speeds in the boundary current at the depth of the sensors used here are on the order of 15 $cm\,s^{-1}$ (Zantopp et al., 2017), and the distance to the region where the interior convection area is closest to the 3000 m isobath is about 450 km (see Fig. 7). The time scale for LSW to arrive at the 53° N moorings after entering the boundary current would therefore be about 35 days. This is consistent with the time lag of approximately one month between the seasonal cycle of LSW input

https://doi.org/10.5194/bg-2021-185
Preprint. Discussion started: 3 August 2021

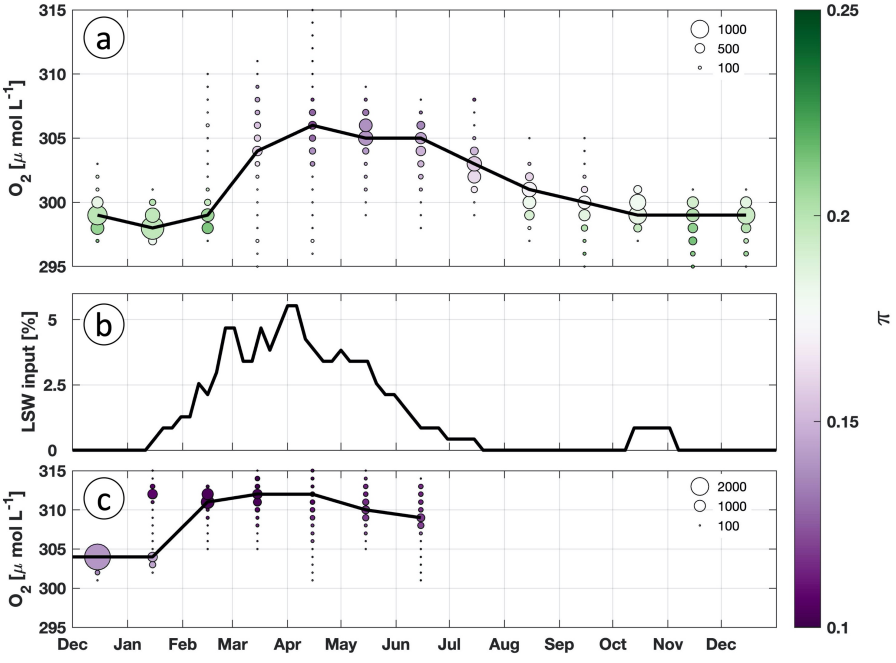

Figure 9. a) Monthly histogram of oxygen from December 2016 to December 2017 at 610 m depth at K9, as in Fig. 8. The size of each circle corresponds to the number of observations, the black line shows the bin with the highest number of observations for each month, and colors show the mean spiciness of each O_2 bin.

b) Climatological seasonal cycle of LSW input into the boundary current from float data in 5-day bins, as a fraction of the total input of LSW over the year. LSW input is defined to include both LSW exported from the interior and convection within the boundary current. The time series is smoothed with a 5-point running mean.

c) Monthly histogram of oxygen from December 2016 to July 2017 at 500 m depth for the SeaCycler mooring in the deep convection area in the interior of the basin. The size of each circle corresponds to the number of observations, the black line shows the bin with the highest number of observations for each month, and colors show the mean spiciness of each O_2 bin.

and the O_2 maximum time series at the K9 mooring. The data therefore support the hypothesis that the increase in oxygen concentration at the exit of the basin is largely controlled by the rate of formation and subsequent export of LSW.

255 If the bulk of the LSW arriving at 53° N originates in the center of the basin near the SeaCycler mooring, the time difference between the oxygen increase at SeaCycler and the increased LSW input into the boundary current implies a mean advection speed of 9 $\mathrm{cm\,s^{-1}}$. This is much larger than the climatological advection speed in the interior (see Fig. 1), suggesting that short-lived features such as eddies and current meanders may play a crucial role in the export of newly formed LSW.

https://doi.org/10.5194/bg-2021-185
Preprint. Discussion started: 3 August 2021

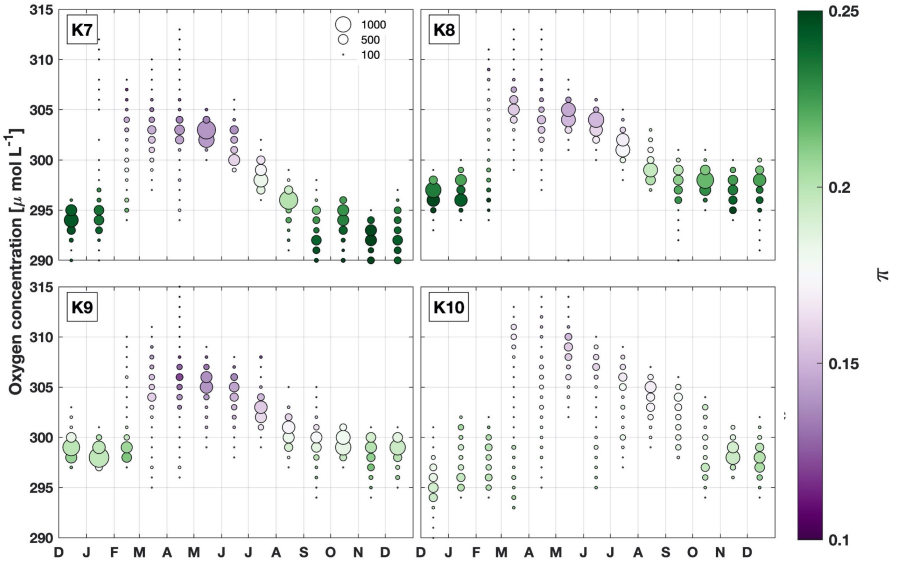

Figure 10. Monthly oxygen histograms as in Figure 8a, for all four moorings. Circle size corresponds to number of observations, and colors show the mean spiciness (π) in each bin, highlighting the relative influence of IW and LSW.

3.3 Differences at the 53° N array

Although the seasonal oxygen cycle at K9 discussed in the previous section is representative of the general picture along the 53° N array, there are also some horizontal differences. The four moorings that carry oxygen sensors are deployed in different parts of the boundary current system at the exit of the Labrador Sea. The K9 mooring, discussed in the previous section, is situated within the core of the Deep Western Boundary Current (DWBC), which has only a weak velocity shear between 400 m and 2000 m (Zantopp et al., 2017). K7 sits over the continental shelf beneath the core of the Labrador Current (LC), which is surface intensified, and carries colder, fresher water of Arctic origin. The K8 sensors at 600 m depth are within the DWBC, but closer to the boundary with the LC, and can be within it when the currents are meandering. At all three of these moorings, the flow is southward, with mean velocities over the deployment period between -13 $\mathrm{cm\,s^{-1}}$ and -15 $\mathrm{cm\,s^{-1}}$. In contrast, the K10 mooring is at the boundary between the offshore edge of the DWBC and its northward recirculation. Over the deployment period, there is a weak mean northward flow at about 600 m, with a speed of 3.5 $\mathrm{cm\,s^{-1}}$, but daily mean values are distributed evenly around this mean, ranging from -20 $\mathrm{cm\,s^{-1}}$ to +20 $\mathrm{cm\,s^{-1}}$. The seasonal cycle of oxygen concentrations at all four moorings (Fig. 10) shows elevated values and water with properties closer to LSW during spring and summer, and water with lower oxygen values resembling IW in autumn and winter.

At the border of the Labrador Current and DWBC, the oxygen concentrations measured at K8 show a similar seasonal cycle as those at K9. Properties measured by the water mass index (π) are also comparable, although the spread in T and S is higher (Fig. 5), suggesting that the DWBC here is less homogenized than at K9.

https://doi.org/10.5194/bg-2021-185
Preprint. Discussion started: 3 August 2021

Over the continental slope at K7, the oxygen concentration is lower by about 5 $\mu\mathrm{mol\,L^{-1}}$ throughout the year, and the earliest high-oxygen measurements already occur in January rather than February. The water is generally warmer and fresher than at the other moorings, which may be the reason for the lower oxygen values, and also results in a slightly lower mean density. Unlike for K9, there seems to be a stronger seasonal variability in density: Between the warmer, saltier, oxygen-poor water in winter and the high-oxygen, low T/S water in spring, density increases by more than 0.05 $\mathrm{kg\,m^{-3}}$ (Fig. 5). This is similar to variability observed upstream in the boundary current near 55° N by Cuny et al. (2005), who showed that this is a result of isopycnals steepening in winter over the continental slope. This weakened stratification may allow for the formation of uLSW (Pickart et al., 1997). At K7, the highest oxygen concentrations occur at lower densities and salinities, seen as a "tail" in the bottom left corner of the T/S plot. Moreover, the first high-oxygen measurements occur almost three weeks earlier than at K9, which may suggest that these are a product of formation of uLSW within the Labrador Current, and that this formation takes place closer to the mooring section than the production of classical LSW found at the other moorings. Since Argo floats generally stay offshore of the 2000 m isobath, formation of uLSW within the Labrador Current would be difficult to detect with the methods used in Sect. 3.1.

At the offshore edge of the southward boundary current, at mooring K10, the oxygen concentrations are more spread out, and elevated values are not found until the beginning of March. The spread of oxygen concentrations measured during any given month is much larger than for the other moorings, and the T/S signature of the two different water masses is less pronounced. This is likely a result of current meanders, with the mooring measuring the DWBC some of the time and its recirculation at other times, resulting in a wider range of ventilation timescales. There is no significant correlation between oxygen concentrations and southward current speed ($R^2 = 0.006$), suggesting that high O_2 water at K10 is carried southward with the offshore edge of the DWBC, but also recirculated northward back towards the Labrador Sea.

4 Discussion

4.1 LSW formation and export pathways

The analysis in Sect. 3.1 shows that deep mixed layers associated with convection are more commonly found in the interior. In Fig. 7, the area where more than 5% of profiles measure mixed layers deeper than 600 m is about 15 times larger in the interior than inshore of the 3000 m isobath. However, this does not necessarily translate to 15 times larger oxygen supply, as water parcels have a longer residence time in the interior, whereas newly formed LSW in the boundary current is rapidly exported (MacGilchrist et al., 2020, 2021). This is also evident in our data analysis, where a significant number of Argo floats measuring deep mixed layers in the interior do not enter the boundary current during the same season, and therefore do not directly contribute to the oxygen export by the outflowing boundary current. Moreover, LSW formation within the boundary current can also occur as slantwise convection (Cuny et al., 2005), or in parts of the boundary current that are shallower than 2000 m, neither of which would be detectable with Argo floats. As discussed in Sect. 3.3, some evidence of convection over the continental slope upstream can be seen in data from the K7 mooring, at a water depth of 1400 m. However, neither the mooring data, which do not measure local convection, nor the Argo data, biased towards sampling regions with mild currents at

https://doi.org/10.5194/bg-2021-185
Preprint. Discussion started: 3 August 2021

depth, provide sufficient information to quantitatively determine the portion of the LSW exported at 53° N that is formed in the boundary current. The importance of boundary versus interior convection for the outflowing LSW remains an open question, with one previous estimate from float data concluding that both could be important for the properties of the outflowing boundary current (Palter et al., 2008).

Another crucial aspect concerning the export of LSW from the formation region is how the water formed in the interior enters the boundary current. Palter et al. (2008) showed that both eddies and a mean cross-isobath flow can contribute to LSW export, with floats entering the boundary current on all sides of the basin, which is also the case for the float data used here (not shown). The time scale for a water parcel to round the basin from Cape Farewell to the Labrador side is about 147 days (Cuny et al., 2002). This implies that LSW entering the boundary current, or formed within it, on the northern side of the basin during the height of convection in March would not reach 53° N until August, when the influence of LSW at K9 is already decreasing. Thus, the outflow of LSW during summertime observed at 53° N is likely fed mostly by LSW entering the boundary current on the western or southwestern side, allowing for faster export out of the basin. The timing of the seasonal cycles of oxygen concentration in the interior, LSW input into the boundary current, and oxygen concentration at K9 (Fig. 9) implies that eddies may play an important role in exchanging water between the boundary current and interior, consistent with previous studies (Eden and Böning, 2002; Straneo, 2006; de Jong et al., 2014).

In a recent study, Georgiou et al. (2020) used model data to analyze the source of water parcels reaching the 53° N section, and found that 41% did not leave the boundary current after passing Cape Farewell at the southern tip of Greenland, while a further 44% are modified in the interior of the basin before re-entering the boundary current, and the remainder follow several less common pathways. These numbers are broadly consistent with the results from Fig. 8, with about equal amounts of LSW and IW found at the moorings over an annual cycle. Our study suggests that there may be a seasonal dependence to the split observed by Georgiou et al. (2020), with the LSW export (interior route) occurring chiefly in the months following the onset of convection, and IW (water from Cape Farewell) being more ubiquitous during autumn and winter. The export of newly ventilated LSW in the months following convection observed here is consistent with the more direct southward export of lighter LSW found in their study, as well as results from an earlier modeling study (Brandt et al., 2007). Georgiou et al. (2020) suggested that pathways are different for the densest LSW formed in the interior, with water entering the boundary current on the northern side of the basin, thus taking longer to reach 53° N. This density dependence may explain why most of the LSW found in the mooring record seems to follow the faster southward export route, as the lower part of the LSW layer is not sampled in the current sensor setup. Another model study by Handmann (2019) highlighted different routes that exist for LSW export, including several pathways for LSW entering the Irminger Sea. Their study also proposes that some of the water exported through the 53° N section subsequently leaves the DWBC at Orphan Knoll near 50° N and recirculates back towards the north, reaching both the Labrador and Irminger Seas. In our data from the mooring furthest offshore, K10, there is evidence of high-oxygen water with northward velocities (Sect. 3.3), suggesting that newly formed LSW is also entrained into this northward recirculation.

These studies show that many more LSW export pathways exist in addition to the direct southward route that seems to be responsible for the pronounced seasonal signal at the 53° N moorings. Although the large summertime increase in oxygen (Fig.

https://doi.org/10.5194/bg-2021-185
Preprint. Discussion started: 3 August 2021

8) is associated with LSW formed in the same year, the oxygen concentrations will also be impacted by water following these alternative routes. For example, some of the LSW formed in the interior one year may be advected into the Irminger Sea, enter the boundary current on the eastern side of Greenland, and stay within it until it reaches 53° N several years later. Convection also takes place in the Irminger Sea (de Jong et al., 2018), leading to a somewhat weaker, but still significant uptake of oxygen (Maze et al., 2012; Palevsky and Nicholson, 2018). The water mass formed by convection in the Irminger Sea, known there as Irminger Sea Intermediate Water, or ISIW (Le Bras et al., 2020), is what we have referred to here as Irminger Water (IW). Therefore, both the export of LSW into the Irminger Sea and convection occurring there will have affected the properties of the "low-oxygen" IW seen in Fig. 8–10, and the annual minimum concentration of 298 $\mu\mathrm{mol\,L^{-1}}$ at K9 is likely already elevated compared to what it would have been without ventilation in the Labrador and Irminger Seas.

4.2 Global impact of Labrador Sea ventilation

Due to the global importance of LSW, it has long been assumed that changes in its formation would play a crucial role in setting the variability of the Atlantic Meridional Overturning Circulation (Koltermann et al., 1999; Yashayaev, 2007). However, results from the Overturning in the subpolar North Atlantic (OSNAP) program have called into question this long-held belief, showing that the bulk of the water mass transformation across isopycnals occurs east of Greenland in the Irminger Sea and Iceland Basin. This water mass transformation in the eastern section appears to be the main source of overturning variability (Lozier et al., 2019), although recent modelling results suggest that Labrador Sea Water formation may still be important for variability on multidecadal time scales that are not yet resolved by the OSNAP time series (Yeager et al., 2021).

In a recent follow-up study to the OSNAP results, Zou et al. (2020) showed that the disconnect between overturning and LSW formation is in large part due to density-compensated changes in temperature and salinity: Although over 12 Sv of water mass transformation occurs in the Labrador Sea from warm, salty waters to colder and fresher ones, the net transformation into the LSW density range is only about 4 Sv. Our results are consistent with these findings, showing that while the water mass properties of the outflow are altered substantially by the input of newly formed LSW, its density remains largely unchanged. This suggests that LSW from the interior enters the boundary current primarily along isopycnals, consistent with recent results from models (Brüggemann and Katsman, 2019; Georgiou et al., 2020), with some along-isopycnal mixing occurring before it reaches 53° N. Our time series also show for the first time direct evidence that significant changes occur in the oxygen content of the outflow, driven by the rapid export of newly ventilated LSW. While we only use data from a fixed depth, oxygen concentrations in the summer are elevated in much of the LSW layer above 1200 m (Fig. 2). Assuming that the oxygen input is comparable throughout this layer, we can calculate a first estimate of the oxygen transported out of the basin due to the input of newly formed LSW: Using a mean velocity of 15 $\mathrm{cm\,s^{-1}}$, an average layer thickness of 950 m, and a section width of 100 km for the mooring array excluding the recirculation at K10, the oxygen increase of 6 $\mu\mathrm{mol\,L^{-1}}$ at K9 during March–August 2017 relative to the January baseline of 298 $\mu\mathrm{mol\,L^{-1}}$ (Fig. 8) corresponds to a supply of oxygen to the North Atlantic Ocean of 1.35 Tmol (1 Tmol = 10^{12} mol) for these six months, and 1.57 Tmol for the whole year. With an integrated wintertime uptake across the air-sea interface due to gas exchange of 21.2 $\mathrm{mol\,m^2}$ (Atamanchuk et al., 2020) and a convection area of approximately 150,000 $\mathrm{km^2}$, the total uptake in the interior is 3.18 Tmol during the same year. Thus, about 42% of the oxygen

https://doi.org/10.5194/bg-2021-185
Preprint. Discussion started: 3 August 2021

taken up during convection is exported out of the basin via this fast export route of LSW along the DWBC during summer, and another 7% through slower export routes during the rest of the year. As discussed in Sect. 4.1, the overall impact of LSW ventilation on the oxygen supply from the Labrador Sea to the rest of the North Atlantic Ocean may be even larger if other, more indirect, pathways on time scales longer than a year are considered.

The deep North Atlantic is one of the few ocean regions that has not experienced significant deoxygenation in recent decades (Schmidtko et al., 2017), which may be related to the continued formation and export of LSW and NADW. The 1.57 $\mathrm{Tmol\,year^{-1}}$ of export calculated for 53° N are small compared to the recent multidecadal 70 $\mathrm{Tmol\,year^{-1}}$ oxygen loss reported by Schmidtko et al. (2017) for the global deep ocean, but may be sufficient to supply much of the oxygen consumed in this layer in the North Atlantic. With a global mean apparent oxygen utilization rate of 0.1 $\mathrm{\mu mol\,kg^{-1}\,year^{-1}}$ at 1500 m depth (Karstensen et al., 2008), an area of 26,159,000 $\mathrm{km^2}$ for the deep Atlantic Ocean between the equator and 50° N, and a mean layer thickness of 800 m for the isopycnal range 27.68 $\mathrm{kg\,m^{-3}} \leq \sigma_\theta \leq$ 27.8 $\mathrm{kg\,m^{-3}}$, the annual oxygen consumption for this volume of water is 2.2 Tmol. The rapid southward export of LSW discussed here supplies 71% of the oxygen demand in this layer, with the rest likely provided by slower export of LSW through other routes, as well as uptake in other deep water formation regions such as the Irminger Sea (Palevsky and Nicholson, 2018), Iceland basin (Maze et al., 2012), and the Gulf of Lion in the Mediterranean Sea (Ulses et al., 2021). Thus, despite playing a less significant role than previously thought in setting the strength of the overturning (Lozier et al., 2019), convection in the Labrador Sea does appear to crucially contribute to the supply of oxygen from the subpolar North Atlantic to the deep subtropical and tropical Atlantic Ocean. This highlights the important distinction between the overturning circulation and the ventilation of deep waters, as discussed by Naveira Garabato et al. (2017) and MacGilchrist et al. (2020, 2021). Although the density transformation is weaker in the Labrador Sea, there is a more direct connection between the atmosphere and deep ocean during the formation of LSW compared to the water mass formation and transformation processes in the eastern subpolar gyre, allowing for more intense oxygen uptake.

4.3 Outlook

A key topic of research regarding Labrador Sea Water formation is its susceptibility to future climate change. Model studies have suggested that increased freshwater input resulting from the melting of Greenland's ice sheets may weaken or even shut down convection in the Labrador Sea (Manabe and Stouffer, 1997; Rahmstorf, 1999; Clark et al., 2002). While the re-emergence of LSW formation to near record depths in 2014–2016 shows that the effect of ice melt has not yet critically affected convection (Yashayaev and Loder, 2016, 2017), recent climate projections and observations continue to point towards a possible shutdown in the future (Böning et al., 2016; Oltmanns et al., 2018). If convection in the Labrador Sea were to cease, the "trap door" of oxygen uptake to the deep ocean would be shut (Atamanchuk et al., 2020), cutting off a large part of the oxygen supply discussed above. Moreover, since ventilation of LSW can occur without any associated density-space overturning, large changes in oxygen supply are possible even if the overturning circulation remains stable.

In a recent model study on future deep ocean deoxygenation, Oschlies (2021) posited that his work *"calls for more research efforts to explore the baseline of these systems before the unavoidable change will hit"*. The present study represents a first step towards quantifying the impact of LSW formation and export on the supply of oxygen to the open Atlantic Ocean. However,

https://doi.org/10.5194/bg-2021-185
Preprint. Discussion started: 3 August 2021

more measurements will be needed to better understand the complex interplay between different deep water formation regions, and the resulting supply of oxygen associated with ventilation in the subpolar North Atlantic as a whole. To that end, oxygen sensors were added to several moorings in the OSNAP array in 2020, and the 53° N oxygen time series have been continued for an additional 4 years. In total, 70 O_2 sensors are currently deployed along the path of the boundary current in the Irminger Sea, the Labrador Sea near the southern tip of Greenland, and on the 53° N array. With the resulting data, it will become possible to gain a much more complete understanding of the processes controlling oxygen supply from the subpolar North Atlantic than has been presented here.

5 Conclusions

The results put forth in this study show the effect of Labrador Sea Water formation and export on the oxygen concentration of the outflowing deep western boundary current. During autumn and winter, properties measured at the 53° N array at about 600 m nominal depth are similar to those of Irminger Water, which enters the basin from the Irminger Sea. LSW first arrives at the offshore moorings in the second half of February, with a wide range of temperature, salinity, and oxygen properties reflecting a sporadic input of heterogeneous LSW formed in or near the boundary current. As convection becomes more vigorous and sustained, and more newly formed LSW enters the boundary current from the interior, it becomes the dominant water mass found at 53° N in April–May. As a result, the most commonly measured oxygen concentration for these months is 7-8 $\mu\mathrm{mol\,L^{-1}}$ higher than in December and January. By September, the signature of LSW has largely disappeared, and properties once again resemble those of IW, with accordingly lower oxygen concentrations. This suggests that most of the direct southward export of newly formed LSW occurs in the 6 months following convection. However, additional measurements throughout the LSW density range would be needed to evaluate whether the seasonal cycle is the same for the entire layer, or just for the part of it measured with the current sensor setup.

The increase in oxygen content due to the input of LSW into the boundary current amounts to an added oxygen export out of the basin of 1.57 $\mathrm{Tmol\,year^{-1}}$, which is about 49% of the oxygen taken up during convection in the interior. The annual oxygen supply from this fast, direct export of LSW to the Atlantic Ocean is equivalent to 71% of the oxygen demand by organisms in the upper NADW layer of the North Atlantic Ocean, highlighting the crucial role that the Labrador Sea plays in the supply of oxygen to the deep ocean. When taking into account the complex export pathways of LSW through the subpolar gyre, as well as uptake in other deep water formation regions, the overall oxygen export associated with North Atlantic Deep Water formation is likely even higher. More research will be needed to fully quantify the importance of the subpolar North Atlantic for supplying oxygen to the global oceans via the export of NADW, and to determine how susceptible this process could be to climate change.

https://doi.org/10.5194/bg-2021-185
Preprint. Discussion started: 3 August 2021

Data availability. The mooring data used in this study are available from the authors upon request, and will be made freely available online by the time the final article is published. Argo float data were collected and made freely available by the International Argo Program and the national programs that contribute to it. (https://argo.ucsd.edu, https://www.ocean-ops.org).

Author contributions. The manuscript was prepared by JKo, with contributions from all coauthors. DA was responsible for designing the experiment and calibrating the mooring data, and data analysis was carried out by JKo. DW and JKa acquired funding for the project.

Competing interests. The authors declare that they have no conflict of interest.

Acknowledgements. JKo was funded by the Ocean Frontier Institute through the International Postdoctoral Fellowship. This work was funded in part by the Canada Excellence Research Chair in Ocean Science and Technology. This research was undertaken thanks in part to funding from the Canada First Research Excellence Fund, through the Ocean Frontier Institute. The 53° N array is supported by EU H2020 Blue Action (grant #727852), EuroSea (grant #862626), and the German Ministry of Education and Research (RACE Program). The 53° N array is part of the OceanSITES Eulerian time series network. Argo float data were collected and made freely available by the International Argo Program and the national programs that contribute to it. (https://argo.ucsd.edu, https://www.ocean-ops.org). The Argo Program is part of the Global Ocean Observing System. The authors would like to thank Marilena Oltmanns for help with processing the mooring data.

https://doi.org/10.5194/bg-2021-185
Preprint. Discussion started: 3 August 2021

References

Argo: Argo float data and metadata from Global Data Assembly Centre (Argo GDAC) - Snapshot of Argo GDAC of October 10st 2020., https://doi.org/10.17882/42182#77634, 2020.

Atamanchuk, D., Koelling, J., Send, U., and Wallace, D.: Rapid transfer of oxygen to the deep ocean mediated by bubbles, Nature Geoscience, pp. 1–6, https://doi.org/10.1038/s41561-020-0532-2, 2020.

Atkinson, C., Bryden, H., Cunningham, S., and King, B.: Atlantic transport variability at 25° N in six hydrographic sections., Ocean Science, 8, https://doi.org/10.5194/os-8-497-2012, 2012.

Böning, C. W., Behrens, E., Biastoch, A., Getzlaff, K., and Bamber, J. L.: Emerging impact of Greenland meltwater on deepwater formation in the North Atlantic Ocean, Nature Geoscience, 9, 523–527, https://doi.org/10.1038/ngeo2740, 2016.

Bower, A. S., Lozier, M. S., Gary, S. F., and Böning, C. W.: Interior pathways of the North Atlantic meridional overturning circulation, Nature, 459, 243, https://doi.org/10.1038/nature07979, 2009.

Brandt, P., Funk, A., Czeschel, L., Eden, C., and Böning, C. W.: Ventilation and Transformation of Labrador Sea Water and Its Rapid Export in the Deep Labrador Current, Journal of Physical Oceanography, 37, 946 – 961, https://doi.org/10.1175/JPO3044.1, 2007.

Brüggemann, N. and Katsman, C. A.: Dynamics of Downwelling in an Eddying Marginal Sea: Contrasting the Eulerian and the Isopycnal Perspective, Journal of Physical Oceanography, 49, 3017 – 3035, https://doi.org/10.1175/JPO-D-19-0090.1, 2019.

Clark, P. U., Pisias, N. G., Stocker, T. F., and Weaver, A. J.: The role of the thermohaline circulation in abrupt climate change, Nature, 415, 863–869, https://doi.org/10.1038/415863a, 2002.

Cuny, J., Rhines, P. B., Niiler, P. P., and Bacon, S.: Labrador Sea Boundary Currents and the Fate of the Irminger Sea Water, Journal of Physical Oceanography, 32, 627 – 647, https://doi.org/10.1175/1520-0485(2002)032<0627:LSBCAT>2.0.CO;2, 2002.

Cuny, J., Rhines, P. B., Schott, F., and Lazier, J.: Convection above the Labrador Continental Slope, Journal of Physical Oceanography, 35, 489 – 511, https://doi.org/10.1175/JPO2700.1, 2005.

de Jong, M. F., Bower, A. S., and Furey, H. H.: Two Years of Observations of Warm-Core Anticyclones in the Labrador Sea and Their Seasonal Cycle in Heat and Salt Stratification, Journal of Physical Oceanography, 44, 427 – 444, https://doi.org/10.1175/JPO-D-13-070.1, 2014.

de Jong, M. F., Oltmanns, M., Karstensen, J., and de Steur, L.: Deep Convection in the Irminger Sea Observed with a Dense Mooring Array, Oceanography, 31, 50–59, http://www.jstor.org/stable/26307787, 2018.

Eden, C. and Böning, C.: Sources of Eddy Kinetic Energy in the Labrador Sea, Journal of Physical Oceanography, 32, 3346 – 3363, https://doi.org/10.1175/1520-0485(2002)032<3346:SOEKEI>2.0.CO;2, 2002.

Fischer, J., Karstensen, J., Oltmanns, M., and Schmidtko, S.: Mean circulation and EKE distribution in the Labrador Sea Water level of the subpolar North Atlantic, Ocean Science, 14, 1167–1183, https://doi.org/10.5194/os-14-1167-2018, 2018.

Flament, P.: A state variable for characterizing water masses and their diffusive stability: spiciness, Progress in Oceanography, 54, 493–501, https://doi.org/10.1016/S0079-6611(02)00065-4, 2002.

Garcia, H. E. and Gordon, L. I.: Oxygen solubility in seawater: Better fitting equations, Limnology and Oceanography, 37, 1307–1312, https://doi.org/10.4319/lo.1992.37.6.1307, 1992.

Georgiou, S., Ypma, S. L., Brüggemann, N., Sayol, J.-M., van der Boog, C. G., Spence, P., Pietrzak, J. D., and Katsman, C. A.: Direct and indirect pathways of convected water masses and their impacts on the overturning dynamics of the Labrador Sea, Journal of Geophysical Research: Oceans, n/a, e2020JC016 654, https://doi.org/10.1029/2020JC016654, 2020.

https://doi.org/10.5194/bg-2021-185
Preprint. Discussion started: 3 August 2021

Handmann, P.: Deep Water Formation and Spreading Dynamics in the subpolar North Atlantic from Observations and high-resolution Ocean Models, Ph.D. thesis, Christian-Albrechts-Universität Kiel, 2019.

Holte, J., Talley, L. D., Gilson, J., and Roemmich, D.: An Argo mixed layer climatology and database, Geophysical Research Letters, 44, 5618–5626, https://doi.org/10.1002/2017GL073426, 2017.

Karstensen, J.: Calibration of physical data, Tech. rep., Internal Report: Animate Report, 2005.

Karstensen, J., Stramma, L., and Visbeck, M.: Oxygen minimum zones in the eastern tropical Atlantic and Pacific oceans, Progress in Oceanography, 77, 331–350, https://doi.org/10.1016/j.pocean.2007.05.009, 2008.

Kieke, D., Rhein, M., Stramma, L., Smethie, W. M., LeBel, D. A., and Zenk, W.: Changes in the CFC Inventories and Formation Rates of Upper Labrador Sea Water, 1997–2001, Journal of Physical Oceanography, 36, 64 – 86, https://doi.org/10.1175/JPO2814.1, 2006.

Koelling, J., Wallace, D. W. R., Send, U., and Karstensen, J.: Intense oceanic uptake of oxygen during 2014–2015 winter convection in the Labrador Sea, Geophysical Research Letters, 44, 7855–7864, https://doi.org/10.1002/2017GL073933, 2017.

Koltermann, K., Sokov, A., Tereschenkov, V., Dobroliubov, S., Lorbacher, K., and Sy, A.: Decadal changes in the thermohaline circulation of the North Atlantic, Deep Sea Research Part II: Topical Studies in Oceanography, 46, 109–138, https://doi.org/10.1016/S0967-0645(98)00115-5, 1999.

Lazier, J.: The renewal of Labrador sea water, Deep Sea Research and Oceanographic Abstracts, 20, 341 – 353, https://doi.org/10.1016/0011-7471(73)90058-2, 1973.

Le Bras, I. A., Yashayaev, I., and Toole, J. M.: Tracking Labrador Sea Water property signals along the Deep Western Boundary Current, Journal of Geophysical Research: Oceans, 122, 5348–5366, https://doi.org/10.1002/2017JC012921, 2017.

Le Bras, I. A.-A., Straneo, F., Holte, J., de Jong, M. F., and Holliday, N. P.: Rapid Export of Waters Formed by Convection Near the Irminger Sea's Western Boundary, Geophysical Research Letters, 47, e2019GL085 989, https://doi.org/10.1029/2019GL085989, 2020.

Lebedev, K. V., Yoshinari, H., Maximenko, N. A., and Hacker, P. W.: Velocity data assessed from trajectories of Argo floats at parking level and at the sea surface, IPRC Technical Note, 4, 1–16, 2007.

Lozier, M. S.: Deconstructing the conveyor belt, Science, 328, 1507–1511, https://doi.org/10.1126/science.1189250, 2010.

Lozier, M. S., Bacon, S., Bower, A. S., Cunningham, S. A., de Jong, M. F., de Steur, L., deYoung, B., Fischer, J., Gary, S. F., Greenan, B. J. W., Heimbach, P., Holliday, N. P., Houpert, L., Inall, M. E., Johns, W. E., Johnson, H. L., Karstensen, J., Li, F., Lin, X., Mackay, N., Marshall, D. P., Mercier, H., Myers, P. G., Pickart, R. S., Pillar, H. R., Straneo, F., Thierry, V., Weller, R. A., Williams, R. G., Wilson, C., Yang, J., Zhao, J., and Zika, J. D.: Overturning in the Subpolar North Atlantic Program: A New International Ocean Observing System, Bulletin of the American Meteorological Society, 98, 737–752, https://www.jstor.org/stable/26243715, 2017.

Lozier, M. S., Li, F., Bacon, S., Bahr, F., Bower, A. S., Cunningham, S. A., de Jong, M. F., de Steur, L., deYoung, B., Fischer, J., Gary, S. F., Greenan, B. J. W., Holliday, N. P., Houk, A., Houpert, L., Inall, M. E., Johns, W. E., Johnson, H. L., Johnson, C., Karstensen, J., Koman, G., Le Bras, I. A., Lin, X., Mackay, N., Marshall, D. P., Mercier, H., Oltmanns, M., Pickart, R. S., Ramsey, A. L., Rayner, D., Straneo, F., Thierry, V., Torres, D. J., Williams, R. G., Wilson, C., Yang, J., Yashayaev, I., and Zhao, J.: A sea change in our view of overturning in the subpolar North Atlantic, Science, 363, 516–521, https://doi.org/10.1126/science.aau6592, 2019.

MacGilchrist, G. A., Johnson, H. L., Marshall, D. P., Lique, C., Thomas, M., Jackson, L. C., and Wood, R. A.: Locations and Mechanisms of Ocean Ventilation in the High-Latitude North Atlantic in an Eddy-Permitting Ocean Model, Journal of Climate, 33, 10 113 – 10 131, https://doi.org/10.1175/JCLI-D-20-0191.1, 2020.

MacGilchrist, G. A., Johnson, H. L., Lique, C., and Marshall, D. P.: Demons in the North Atlantic: Variability of Deep Ocean Ventilation, Geophysical Research Letters, 48, e2020GL092 340, https://doi.org/10.1029/2020GL092340, 2021.

https://doi.org/10.5194/bg-2021-185
Preprint. Discussion started: 3 August 2021

Manabe, S. and Stouffer, R. J.: Coupled ocean-atmosphere model response to freshwater input: Comparison to Younger Dryas Event, Paleoceanography, 12, 321–336, https://doi.org/10.1029/96PA03932, 1997.

Marshall, J. and Schott, F.: Open-ocean convection: Observations, theory, and models, Reviews of Geophysics, 37, 1–64, https://doi.org/10.1029/98RG02739, 1999.

Maze, G., Mercier, H., Thierry, V., Memery, L., Morin, P., and Perez, F. F.: Mass, nutrient and oxygen budgets for the northeastern Atlantic Ocean, Biogeosciences, 9, 4099–4113, https://doi.org/10.5194/bg-9-4099-2012, 2012.

Molinari, R. L., Fine, R. A., Wilson, W. D., Curry, R. G., Abell, J., and McCartney, M. S.: The arrival of recently formed Labrador sea water in the Deep Western Boundary Current at 26.5°N, Geophysical Research Letters, 25, 2249–2252, https://doi.org/10.1029/98GL01853, 1998.

Naveira Garabato, A. C., MacGilchrist, G. A., Brown, P. J., Evans, D. G., Meijers, A. J., and Zika, J. D.: High-latitude ocean ventilation and its role in Earth's climate transitions, Philosophical Transactions of the Royal Society A, 375, 20160324, https://doi.org/10.1098/rsta.2016.0324, 2017.

Oltmanns, M., Karstensen, J., and Fischer, J.: Increased risk of a shutdown of ocean convection posed by warm North Atlantic summers, Nature Climate Change, 8, 300–304, https://doi.org/10.1038/s41558-018-0105-1, 2018.

Oschlies, A.: A committed fourfold increase in ocean oxygen loss, Nature Communications, 12, 1–8, https://doi.org/10.1038/s41467-021-22584-4, 2021.

Pacini, A., Pickart, R. S., Bahr, F., Torres, D. J., Ramsey, A. L., Holte, J., Karstensen, J., Oltmanns, M., Straneo, F., Bras, I. A. L., Moore, G. W. K., and de Jong, M. F.: Mean Conditions and Seasonality of the West Greenland Boundary Current System near Cape Farewell, Journal of Physical Oceanography, 50, 2849 – 2871, https://doi.org/10.1175/JPO-D-20-0086.1, 2020.

Palevsky, H. I. and Nicholson, D. P.: The North Atlantic Biological Pump: Insights from the ocean observatories initiative Irminger Sea Array, Oceanography, 31, 42–49, http://www.jstor.org/stable/26307786, 2018.

Palter, J. B., Lozier, M. S., and Lavender, K. L.: How Does Labrador Sea Water Enter the Deep Western Boundary Current?, Journal of Physical Oceanography, 38, 968 – 983, https://doi.org/10.1175/2007JPO3807.1, 2008.

Pickart, R. S., Spall, M. A., and Lazier, J. R.: Mid-depth ventilation in the western boundary current system of the sub-polar gyre, Deep Sea Research Part I: Oceanographic Research Papers, 44, 1025–1054, https://doi.org/10.1016/S0967-0637(96)00122-7, 1997.

Pickart, R. S., Torres, D. J., and Clarke, R. A.: Hydrography of the Labrador Sea during Active Convection, Journal of Physical Oceanography, 32, 428 – 457, https://doi.org/10.1175/1520-0485(2002)032<0428:HOTLSD>2.0.CO;2, 2002.

Rahmstorf, S.: Shifting seas in the greenhouse?, Nature, 399, 523–524, https://doi.org/10.1038/21066, 1999.

Rhein, M., Fischer, J., Smethie, W. M., Smythe-Wright, D., Weiss, R. F., Mertens, C., Min, D.-H., Fleischmann, U., and Putzka, A.: Labrador Sea Water: Pathways, CFC Inventory, and Formation Rates, Journal of Physical Oceanography, 32, 648 – 665, https://doi.org/10.1175/1520-0485(2002)032<0648:LSWPCI>2.0.CO;2, 2002.

Rhein, M., Walter, M., Mertens, C., Steinfeldt, R., and Kieke, D.: The circulation of North Atlantic Deep Water at 16°N, 2000–2003, Geophysical Research Letters, 31, https://doi.org/10.1029/2004GL019993, 2004.

Rieck, J. K., Böning, C. W., and Getzlaff, K.: The Nature of Eddy Kinetic Energy in the Labrador Sea: Different Types of Mesoscale Eddies, Their Temporal Variability, and Impact on Deep Convection, Journal of Physical Oceanography, 49, 2075 – 2094, https://doi.org/10.1175/JPO-D-18-0243.1, 2019.

Roemmich, D., Johnson, G. C., Riser, S., Davis, R., Gilson, J., Owens, W. B., Garzoli, S. L., Schmid, C., and Ignaszewski, M.: The Argo Program: Observing the Global Ocean with Profiling Floats, Oceanography, 22, 34–43, http://www.jstor.org/stable/24860957, 2009.

https://doi.org/10.5194/bg-2021-185
Preprint. Discussion started: 3 August 2021

Schmidtko, S., Stramma, L., and Visbeck, M.: Decline in global oceanic oxygen content during the past five decades, Nature, 542, 335–339, https://doi.org/10.1038/nature21399, 2017.

Smith, W. H. F. and Sandwell, D. T.: Global Sea Floor Topography from Satellite Altimetry and Ship Depth Soundings, Science, 277, 1956–1962, https://doi.org/10.1126/science.277.5334.1956, 1997.

Straneo, F.: Heat and Freshwater Transport through the Central Labrador Sea, Journal of Physical Oceanography, 36, 606 – 628, https://doi.org/10.1175/JPO2875.1, 2006.

Straneo, F., Pickart, R. S., and Lavender, K.: Spreading of Labrador sea water: an advective-diffusive study based on Lagrangian data, Deep Sea Research Part I: Oceanographic Research Papers, 50, 701–719, https://doi.org/10.1016/S0967-0637(03)00057-8, 2003.

Sy, A., Rhein, M., Lazier, J. R., Koltermann, K. P., Meincke, J., Putzka, A., and Bersch, M.: Surprisingly rapid spreading of newly formed intermediate waters across the North Atlantic Ocean, Nature, 386, 675–679, https://doi.org/10.1038/386675a0, 1997.

Talley, L. and McCartney, M.: Distribution and Circulation of Labrador Sea Water, J. Phys. Oceanography, 1, https://doi.org/10.1175/1520-0485(1982)012<1189:DACOLS>2.0.CO;2, 1982.

Tengberg, A. and Hovdenes, J.: Information on long-term stability and accuracy of Aanderaa oxygen optodes; information about multipoint calibration system and sensor option overview, Aanderaa Data Instruments AS Tech. Note, 14, 2014.

Tengberg, A., Hovdenes, J., Andersson, H. J., Brocandel, O., Diaz, R., Hebert, D., Arnerich, T., Huber, C., Körtzinger, A., Khripounoff, A., Rey, F., Rönning, C., Schimanski, J., Sommer, S., and Stangelmayer, A.: Evaluation of a lifetime-based optode to measure oxygen in aquatic systems, Limnology and Oceanography: Methods, 4, 7–17, https://doi.org/10.4319/lom.2006.4.7, 2006.

Toole, J. M., Andres, M., Le Bras, I. A., Joyce, T. M., and McCartney, M. S.: Moored observations of the Deep Western Boundary Current in the NW Atlantic: 2004-2014, Journal of Geophysical Research: Oceans, 122, 7488–7505, https://doi.org/10.1002/2017jc012984, 2017.

Ulses, C., Estournel, C., Fourrier, M., Coppola, L., Kessouri, F., Lefèvre, D., and Marsaleix, P.: Oxygen budget of the north-western Mediterranean deep-convection region, Biogeosciences, 18, 937–960, https://doi.org/10.5194/bg-18-937-2021, 2021.

Wolf, M. K., Hamme, R. C., Gilbert, D., Yashayaev, I., and Thierry, V.: Oxygen Saturation Surrounding Deep Water Formation Events in the Labrador Sea From Argo-O2 Data, Global Biogeochemical Cycles, 32, 635–653, https://doi.org/10.1002/2017GB005829, 2018.

Yashayaev, I.: Hydrographic changes in the Labrador Sea, 1960-2005, Progress in Oceanography, 75, https://doi.org/10.1016/j.pocean.2007.04.015, 2007.

Yashayaev, I. and Loder, J. W.: Recurrent replenishment of Labrador Sea Water and associated decadal-scale variability, Journal of Geophysical Research: Oceans, 121, 8095–8114, https://doi.org/10.1002/2016JC012046, 2016.

Yashayaev, I. and Loder, J. W.: Further intensification of deep convection in the Labrador Sea in 2016, Geophysical Research Letters, 44, 1429–1438, https://doi.org/10.1002/2016GL071668, 2017.

Yeager, S., Castruccio, F., Chang, P., Danabasoglu, G., Maroon, E., Small, J., Wang, H., Wu, L., and Zhang, S.: An Outsized Role for the Labrador Sea in the Multidecadal Variability of the Atlantic Overturning Circulation, EarthArXiv [preprint], https://doi.org/10.31223/X5ZP68, 2021.

Zantopp, R., Fischer, J., Visbeck, M., and Karstensen, J.: From interannual to decadal: 17 years of boundary current transports at the exit of the Labrador Sea, Journal of Geophysical Research: Oceans, 122, 1724–1748, https://doi.org/10.1002/2016JC012271, 2017.

Zou, S., Lozier, M. S., Li, F., Abernathey, R., and Jackson, L.: Density-compensated overturning in the Labrador Sea, Nature Geoscience, 13, 121–126, https://doi.org/10.1038/s41561-019-0517-1, 2020.

Zunino, P., Mercier, H., and Thierry, V.: Why did deep convection persist over four consecutive winters (2015–2018) southeast of Cape Farewell?, Ocean Science, 16, 99–113, https://doi.org/10.5194/os-16-99-2020, 2020.